

# Proton Induced Nuclide Production Cross Section by HETC-3STEP/FRG-R

Nobuhiro SHIGYO, Kenji ISHIBASHI, Nobuaki YOSHIZAWA\* and Hiroshi TAKADA\*\*

*Department of Nuclear Engineering, Kyushu University  
Hakozaki, Higashi-ku, Fukuoka-shi 812-81, Japan*

*\* Mitsubishi Research Institute, Inc.*

*2-3-6 Otemachi, Chiyoda-ku, Tokyo 100, Japan*

*\*\* Japan Atomic Energy Research Institute*

*Tokai-mura, Ibaraki-ken 319-11, Japan*

*mailto:shigyo@kune2a.nucl.kyushu-u.ac.jp*

High Energy Transport Code (HETC) based on the intranuclear-cascade-evaporation model is modified to calculate the fragmentation cross section. The exciton model is adopted for improvement of backward nucleon-emission cross section for low-energy nucleon-incident events. The level density parameter depending on the excitation energy is taken in the evaporation process. The fragmentation reaction is incorporated into HETC as a subroutine set by the use of the systematics of the reaction. The modified HETC (HETC-3STEP/FRG-R) reproduces experimental fragment yields to a reasonable degree.

## 1. Introduction

Reliable high-energy nuclear data are necessary for application of the spallation reaction to facilities such as the high intensity neutron source [2] and the accelerator based transmutation [1]. Cross sections of the fragmentation reaction which is induced by incident nucleons of energies above several hundred MeV are required for engineering design. Since it is difficult to obtain the whole fragmentation data by experiments, calculation models need to be developed.

High Energy Transport Code (HETC) [3] is currently often used for engineering purposes at intermediate energies. The code mainly considers the intranuclear-cascade and evaporation processes in the nuclear-reaction part. The production yields of the fragments such as  ${}^7\text{Be}$  and  ${}^{24}\text{Na}$  are not represented by HETC, since the fragmentation process is not taken into consideration. We, therefore, have modified this code as HETC-FRG to calculate the intermediate-energy proton-incident fragmentation cross sections. The nuclear in-medium correction is taken into account in the intranuclear-cascade process.

For further improvement of the code, the exciton model is adopted for better reproduction of the nucleon emission cross sections for nucleon-incident at low energies. This code is named as HETC-3STEP/FRG. To improve production cross sections of the nuclei near the target nucleus, the level density parameter depending on the excitation energy is used in the evaporation process. This code is designated HETC-3STEP/FRG-R.

## 2. Fragmentation Process

Before incorporation of the proton-incident fragmentation process into HETC, systematics on the mass yields and the kinetic energy spectra of the process have been constructed [6]. The former was obtained on the basis of a liquid-gas phase transition model [7], and was parameterized by the incident proton energy, the target and the fragment mass numbers and the fragmentation nuclear temperature. For the latter, a formula was devised to have a simple expression considering the Coulomb barrier. The kinetic energy spectra were represented by the parameters of the fragmentation nuclear temperature, the fragment and the target mass numbers and the incident proton energy. The nuclear temperature of the fragmentation was determined in average by the incident proton energy.

For the calculation in HETC, it is assumed that the fragmentation process occurs between the cascade and evaporation processes. The systematics are incorporated with some modification as a subroutine set into HETC [8]. The probability of the fragmentation occurrence is evaluated by the excitation energy after the cascade process, instead of the use of incident proton energy. The nuclear temperature is at first obtained by the fermi gas model after the cascade process without considering a degree of freedom

of the fragmentation: The temperature is given by the excitation energy and the mass number of the nucleus after the cascade process. Then, this temperature is converted into that of the fragmentation. The method takes into account information on the nucleus after the cascade process such as excitation energy and mass number.

The free-space nucleon-nucleon ( $NN$ ) cross sections are used in the intranuclear-cascade process of HETC. Since the  $NN$  collisions occur in the nuclear medium, however, it is important to consider the in-medium correction of  $NN$  cross sections [4]. The  $NN$  cross sections in the intranuclear-cascade process of HETC are modified for this reason. The cross sections in the medium are obtained by simple and practical parameterization [5]. This parameterization is applicable to energies up to 300 MeV. Above 300 MeV, the  $NN$  cross sections in the medium are postulated to increase linearly, and to equal the free-space  $NN$  cross sections at the energy of 500 MeV.

### 3. Exciton Model

The original HETC based on the cascade and evaporation processes is known to underestimate the nucleon emission cross section in the backward direction when incident nucleon energy is around or below 100 MeV. To solve this problem, the exciton model [9] has been adopted as the preequilibrium process between the intranuclear-cascade and the evaporation ones. The model considers the mass and atomic numbers, the excitation energy and the number of the excitons after the intranuclear-cascade process.

The exciton model is effective only in the case that the number of excitons is small, i.e., relatively low excitation energy after the intranuclear-cascade process. On the contrary, the fragmentation tends to occur in a high excitation state, where the number of excitons is larger. At a number of excitons of 15, the calculation is determined to be switched from the process of fragmentation to exciton model. If the number of exciton is below 15, the exciton model calculation follows to the cascade process, whereas the fragmentation process is run if it exceeds 15.

### 4. Level Density Parameter

The level density parameter independent of the excitation energy is used in the evaporation process of the original HETC. The level density parameter depending on the excitation energy [10] is used in HETC-3STEP/FRG to consider the variation of with the excitation energy.

### 5. Calculation Results

Figures 1 to 8 show the production cross sections for  $^{27}\text{Al}$ ,  $^{nat}\text{Fe}$ ,  $^{nat}\text{Zr}$  and  $^{197}\text{Au}$  targets. In these figures  $\bullet$  marks indicate the experimental data [11]. Long-dashed, short-dashed and solid lines stand for the results of HETC-FRG, HETC-3STEP/FRG and HETC-3STEP/FRG-R, respectively. Since the level density parameter dependent on the excitation energy is adopted, HETC-3STEP/FRG-R reproduces the  $^7\text{Be}$  production cross section around 80 MeV region better than HETC-FRG and HETC-3STEP/FRG as shown in Fig. 1. For the reaction of  $^{27}\text{Al}(p, 3pn)^{24}\text{Na}$  in Fig. 2, the cross sections by HETC-3STEP/FRG-R are similar to those by HETC-3STEP/FRG at energies above 40 MeV.

In Fig. 3, each code underestimates the cross sections by a factor of three at proton energies above 400 MeV. The fragmentation process is dominant in the reaction. For the reaction of  $^{nat}\text{Fe}(p, 4pxn)^{48}\text{V}$  in Fig. 4, the cross sections by the three codes are close to the experimental data for the proton incidence above 400 MeV. HETC-3STEP/FRG-R overestimates the cross sections around 20 MeV. The discrepancy indicates the necessity of checking Q-value in the preequilibrium and evaporation processes.

In Fig. 5, the cross sections by the three codes agree with the experimental data because the fragmentation process is dominant in the reaction. For the reaction of  $^{nat}\text{Zr}(p, 4pxn)^{84}\text{Rb}$  in Fig. 6, the cross sections by HETC-3STEP/FRG-R are located between values by HETC-3STEP/FRG and HETC-FRG. This is because the level density parameter depending on the excitation energy is used in the evaporation process of HETC-3STEP/FRG-R. HETC-3STEP/FRG-R overestimates the cross sections around 20 MeV as the reaction of  $^{nat}\text{Fe}(p, 4pxn)^{48}\text{V}$ . The discrepancy also indicates the necessity of checking Q-value in the preequilibrium and evaporation processes.

As shown in Fig. 7, each code represents the production cross section of  $^7\text{Be}$  within a factor of two. The fragmentation process is dominant as in the reactions of  $^{nat}\text{Fe}(p, 23pxn)^7\text{Be}$  and  $^{nat}\text{Zr}(p, 37pxn)^7\text{Be}$ . For the reaction of  $^{197}\text{Au}(p, p3n)^{194}\text{Au}$  in Fig. 8, the results by all codes agree with the experimental data.

## 6. Summary

HETC was modified to calculate the cross section of the proton-incidence fragmentation reaction. The nucleon-nucleon cross sections in the intranuclear-cascade process were changed from free-space to in-medium values. The fragmentation reaction was incorporated into the code as a subroutine set on the basis of the systematics of the proton-induced reaction. The exciton model was taken to improve the nucleon emission cross section in the backward direction. The level density parameter depending on the excitation energy in the evaporation process was adopted. The resultant HETC-3STEP/FRG-R are appropriate to obtain the fragmentation cross sections in the wide target mass range at incident proton energies above several hundred MeV. Although the original HETC is incapable of reproducing the experimental production yields of the light mass fragments like  ${}^7\text{Be}$ , HETC-FRG, HETC-3STEP/FRG, HETC-3STEP/FRG-R represent them to a considerable degree. HETC-3STEP/FRG-R reproduces the  ${}^7\text{Be}$  production cross section around 80 MeV region better than HETC-FRG and HETC-3STEP/FRG.

## References

- [1] Carpenter, J.M., *et al.*: *Proceedings of the twelfth Meeting of International Collaboration on Advanced Neutron Sources 24 - 28 May 1993*, Rutherford Appleton Laboratory Report, 94-025, T-95 (1994).
- [2] Bowman, C.D., *et al.*: *Nucl. Instr. and Meth.*, **A320**, 336 (1992).
- [3] Chandler, K.C., and Armstrong, T.W.: *ORNL 4744* (1972).
- [4] Suetomi, E. *et al.*: *Phys. Lett.*, **B333**, 22 (1994).
- [5] Li, G.Q., and Machleidt, R.: *Phys. Rev.*, **C48**, 1702 (1993); Li, G.Q., and Machleidt, R.: *ibid.*, **C49**, 566 (1994).
- [6] Shigyo, N., *et al.*: *J. Nucl. Sci. Technol.*, **32**, 1 (1995).
- [7] Panagiotou, A.D., *et al.*: *Phys. Rev.*, **C31**, 55 (1985).
- [8] Shigyo, N., *et al.*: *JAERI-Conf.*, **95-008**, 217 (1995); Shigyo, N., *et al.*: *ibid.*, **96-008**, 272 (1995).
- [9] Gudima, K.K., *et al.*: *Nucl. Phys.*, **A401**, 329 (1983).
- [10] Ignatyuk, A.V., *et al.*: *Sov. J. Nucl. Phys.*, **29**, 375 (1979).
- [11] Iljinov, A.S., *et al.*: “*Production of Radionuclides at Intermediate Energies*”, Springer Verlag, Landolt-Bornstein, New Series, subvolumes I/13a (1991), I/13b (1992), I/13c (1993), I/14d (1994).

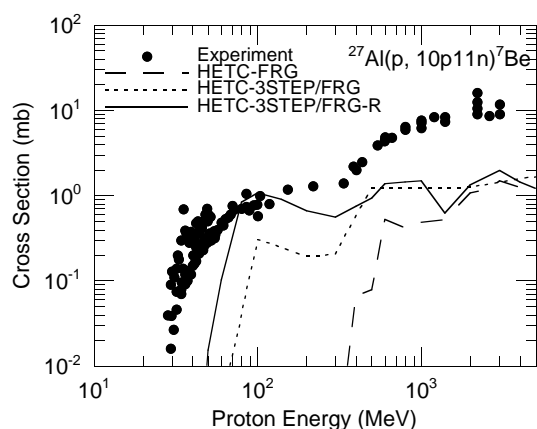


Fig. 1: Production cross section of  ${}^7\text{Be}$  from an Al target.

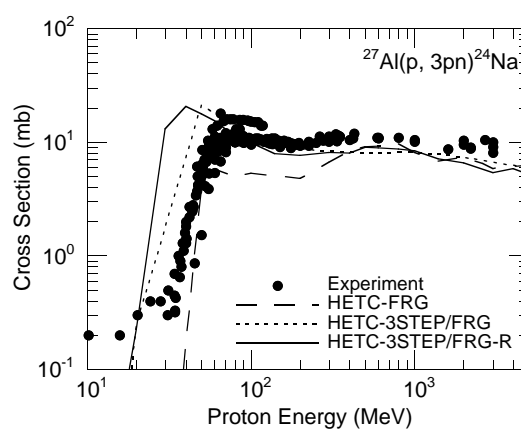


Fig. 2: Production cross section of  ${}^{24}\text{Na}$  from an Al target.

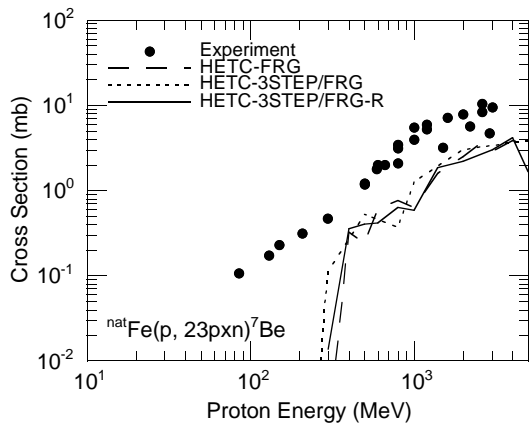


Fig. 3: Production cross section of  $^7\text{Be}$  from an Fe target.

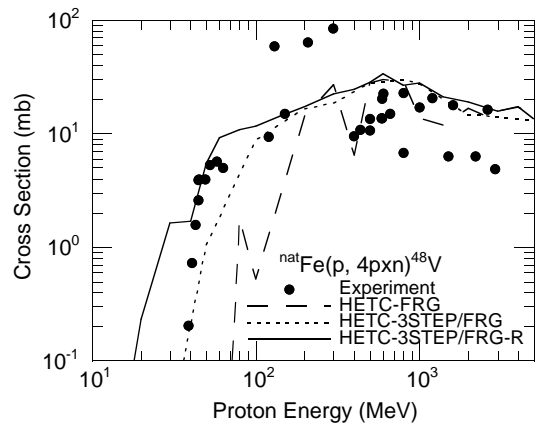


Fig. 4: Production cross section of  $^{48}\text{V}$  from an Fe target.

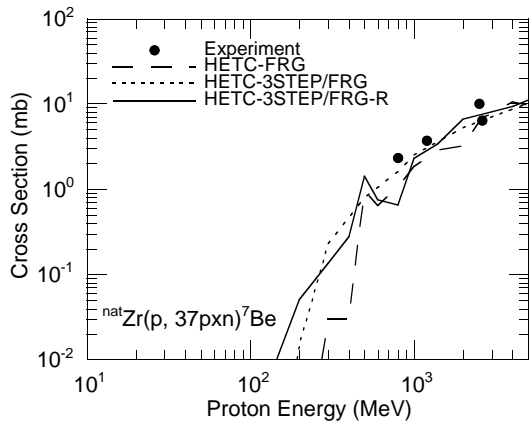


Fig. 5: Production cross section of  $^7\text{Be}$  from a Zr target.

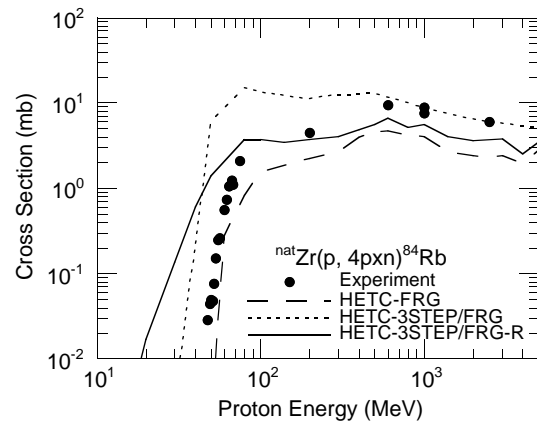


Fig. 6: Production cross section of  $^{84}\text{Rb}$  from a Zr target.

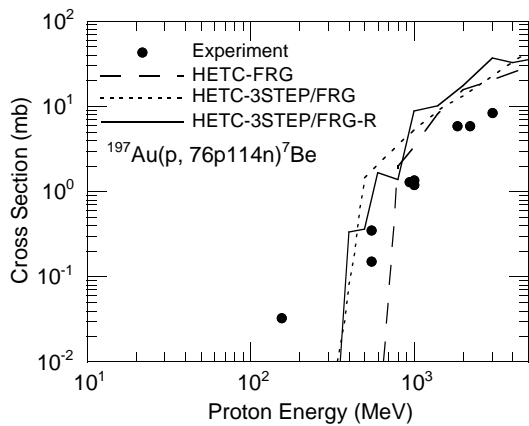


Fig. 7: Production cross section of  $^7\text{Be}$  from an Au target.

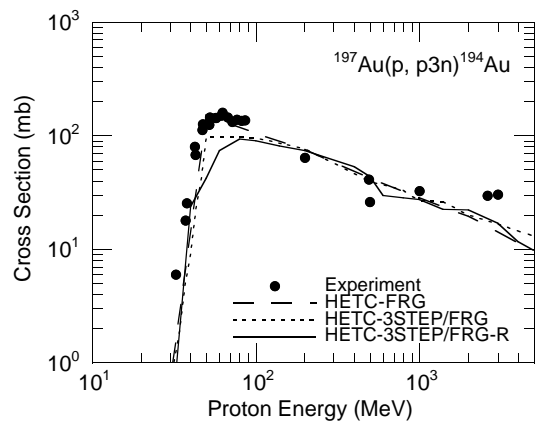


Fig. 8: Production cross section of  $^{194}\text{Au}$  from an Au target.

日本語表題

HETC-3STEP/FRG-R による陽子入射核種生成断面積

著者名

執行信寛、石橋健二、義澤宣明、高田弘